Plasma rotation from momentum transport by neutrals in tokamaks

J Omotani, I Pusztai, T Fülöp
Department of Physics, Chalmers University of Technology, 41296 Gothenburg, Sweden
(Dated: May 6, 2016)

Neutral atoms can strongly influence the intrinsic rotation and radial electric field at the tokamak edge. Here, we present a framework to investigate these effects when the neutrals dominate the momentum transport. We explore the parameter space numerically, using highly flexible model geometries and a state of the art kinetic solver. We find that the most important parameters controlling the toroidal rotation and electric field are the major radius where the neutrals are localized and the plasma collisionality. This offers a means to influence the rotation and electric field by, for example, varying the radial position of the X-point to change the major radius of the neutral peak.

arXiv:1604.08028v2 [physics.plasm-ph] 5 May 2016

The level of plasma rotation has a fundamental impact on the performance of magnetically confined plasmas. Establishing what determines plasma rotation is important both from a theoretical and practical point of view, since rotation has a strong effect on the confinement and stabilizes magnetohydrodynamic instabilities, such as resistive wall modes.

In future magnetic fusion devices, where the effect of alpha-particle heating will be dominant, the external torque from auxiliary heating will be considerably lower than in current devices and the moment of inertia will be higher. It is therefore important to understand the intrinsic toroidal rotation that arises independently of externally applied momentum sources; momentum transport by neutral atoms is a mechanism that generates intrinsic rotation.

There is a wealth of experimental evidence that shows that neutrals have a substantial influence on tokamak edge processes. They are observed to influence global confinement [1, 2] and the transition from low (L) to high (H) confinement mode [3–11], which are critical to the performance of tokamak fusion reactors. While the physics of the transition to H-mode is far from fully understood, it is clear that rotational flow shear plays an important role [12]. It is therefore important to be able to model the effect of neutral viscosity on the flow shear in the edge plasma.

Neutrals influence the ion dynamics in plasmas through atomic processes, mainly through charge-exchange (CX), ionization, and recombination. Due to their high cross-field mobility they can be the most significant momentum transport channel even at low relative densities. The effect of the neutrals is typically significant if the neutral fraction in the plasma exceeds about 10^{-4} [13], which is usually the case in the tokamak edge region not too far inside the separatrix; the neutrals can penetrate even to the pedestal top in the JET tokamak [14] and may be expected to penetrate further in an L-mode plasma due to the lower edge density.

Recent experimental results at JET have demonstrated that changes in divertor strike point positions are correlated with strong modification of the global energy confinement [1, 2]. It was speculated that the reason for this may be that neutrals are directly affecting the edge ion flow and electric potential [1]. Other experimental observations correlate the edge intrinsic toroidal rotation with CX dynamics [14] or the major radius of the X-point [15]. These recent observations triggered renewed interest in the role of the neutrals in the edge region of tokamaks.

Previous analytical work based on neoclassical theory has shown that if the neutral contribution to the toroidal angular momentum is dominant, neutrals can modify or even determine the edge plasma rotation and radial electric field [13, 16–21]. It has been shown that even if there is no input of external momentum into the plasma, the neutrals drive intrinsic momentum transport and hence rotation. The effect of the neutrals is sensitive to their poloidal location which can therefore be used to control the transport. However, analytical solutions for the neoclassical ion distribution function can only be obtained in the asymptotically low or high collisionality regimes. Realistic plasma parameters in the tokamak edge are intermediate between these two limits. The analytical results therefore cannot describe the parametric dependence, for experimentally relevant conditions, of the ion flow and radial electric field or even predict the direction of the trends with, for instance, X-point major radius. By solving the system numerically we can remove the restriction on collisionality and are thus able to model experimentally relevant parameters.

In this paper, we couple neutrals to a neoclassical kinetic solver, allowing us to determine the radial electric field and plasma flows just inside the separatrix. We use ITER-relevant model geometries and plasma parameters. As an example application, we demonstrate the effects of changing the X-point position and the shaping parameters, due to their recent experimental relevance [1, 2, 15]. We will show that there is a link between the X-point radial position and neutral mediated rotation. Consequently, control of the X-point location offers a straightforward means of external control over the ion flow and radial electric field. Our results may have relevance for the mechanism underlying recent observations

indicating improved global confinement with the corner divertor configurations in JET [1, 2].

The toroidal ion flow and radial electric field can be calculated from the steady state condition in a plasma without momentum sources, where the radial transport of toroidal angular momentum should vanish,

$$\left\langle R\hat{\boldsymbol{\zeta}}\cdot(\boldsymbol{\pi}_{\rm i}+\boldsymbol{\pi}_{\rm n})\cdot\nabla\psi\right\rangle = 0. \tag{1}$$

Here $\boldsymbol{\pi}_{\rm i}$ and $\boldsymbol{\pi}_{\rm n}$ are the ion and neutral viscosity tensors, R is the major radius, $2\pi\psi$ is the poloidal magnetic flux, and $\hat{\boldsymbol{\zeta}} = \nabla\zeta/|\nabla\zeta|$ with ζ the toroidal angle in the direction of the plasma current.

For modest relative neutral densities, $n_{\rm n}/n_{\rm i} \gtrsim 10^{-4}$, where $n_{\rm n}$ and $n_{\rm i}$ denote the density of neutrals and ions, it can be shown that the neutral viscosity is higher than the neoclassical viscosity [13]. The turbulent part of the momentum flux will also be assumed to be lower than the neutral momentum flux, which may be questionable. However, it is plausible to think that the neutral and turbulent momentum fluxes should be at least comparable, given the fact that in steady state the particle losses are balanced by fueling and recycling. The neutral particle transport is then equal to ion particle transport due to both collisions *and* turbulence, since every recycling ion that leaves the plasma comes back as a neutral [19]. Therefore considering the neutral momentum transport in isolation is an important step in understanding plasma rotation in regions where neutrals are present. The importance of neutrals for rotation is reinforced by the experimental evidence showing that neutrals do affect plasma rotation at the edge.

We can solve the neutral kinetic equation $\boldsymbol{v}\cdot\nabla f_{\rm n} = \tau^{-1}\left(n_{\rm n}f_{\rm i}/n_{\rm i} - f_{\rm n}\right)$ perturbatively. Here, $\tau^{-1} = n_{\rm i}\langle\sigma v\rangle_x \simeq 2.93 n_{\rm i}\sigma_x(T_i/m_i)^{1/2}$ is the CX frequency, which is much larger than the ionization or recombination rates for tokamak edge parameters. The mean free path for CX is $\lambda_{\rm mfp,n} = \tau v_{\rm th} \simeq 0.483/n_{\rm i}\sigma_x$, with $v_{\rm th}$ the thermal velocity, which we may estimate as $\lambda_{\rm mfp} \simeq 0.8$ cm using $n_{\rm i} = 10^{20}$ m^{-3} and $\sigma_x = 6\times10^{-15}$ cm^2 [13]. This is short compared to typical gradient scale lengths in the plasma, so we expand the neutral distribution function for small $\lambda_{\rm mfp}/L$, where L is a typical gradient scale length, as $f_{\rm n} = f_{\rm n0} + f_{\rm n1} + \ldots$. To lowest order $f_{\rm n0} = n_{\rm n}f_{\rm i}/n_{\rm i}$, and to next order $f_{\rm n1} = -\tau\boldsymbol{v}\cdot\nabla\left(n_{\rm n}f_{\rm i}/n_{\rm i}\right)$. Thus the neutral distribution function can be calculated from the distribution function of the ions. For neutral fractions $n_{\rm n}/n_{\rm i} \lesssim 10^{-3}$, the direct effect of the neutrals on the ion distribution function can be neglected [16], and then we can construct the neutral viscosity tensor as $\pi_{{\rm n},jk} = \int m_{\rm i}\left(v_jv_k - (v^2/3)\delta_{jk}\right)f_{\rm n}(\boldsymbol{v})d^3v = -\tau\frac{\partial}{\partial x_l}\int m_{\rm i}v_jv_kv_l(n_{\rm n}/n_{\rm i})f_{\rm i}(\boldsymbol{v})d^3v + (\ldots)\pi_{{\rm i},jk} + (\ldots)\delta_{jk}$, where the last two terms are negligible compared to the first one, so we have

$$\left\langle R\hat{\boldsymbol{\zeta}}\cdot\boldsymbol{\pi}_{\rm n}\cdot\nabla\psi\right\rangle \approx \left\langle\frac{R\tau m_{\rm i}}{n_{\rm i}}\frac{\partial n_{\rm n}}{\partial\psi}\int d^3v\,\left(\nabla\psi\cdot\boldsymbol{v}\right)^2\left(\hat{\boldsymbol{\zeta}}\cdot\boldsymbol{v}\right)f_{\rm i}\right\rangle, \tag{2}$$

where the radial gradient of $n_{\rm n}$ dominates. Note that even when the neutrals are too few to affect the ion distribution, they still affect the ion toroidal rotation and the radial electric field through the transport of angular momentum. Interestingly, from Eqs. (1) and (2) it follows that the effect does not depend on the magnitude of the neutral density or on the cross section if the neutral viscosity is larger than the ion neoclassical and turbulent viscosities, as long as there are few enough neutrals not to affect the ion distribution function directly.

We calculate the guiding-center ion distribution function $f_{\rm i,gc}$ with the Pedestal and Edge Radially-global Fokker-Planck Evaluation of Collisional Transport (PERFECT) neoclassical solver [22], used here in local mode. In contrast to standard neoclassical calculations which need consider only the guiding center distribution $f_{\rm i,gc}$, the neutrals couple to the *particle* distribution $f_{\rm i}$, given by

$$\begin{aligned} f_{\rm i}(\boldsymbol{r}) &= f^{\rm M}_{\rm i,gc}(\boldsymbol{R}) + \delta f_{\rm i,gc}(\boldsymbol{R}) \\ &\approx f^{\rm M}_{\rm i,gc}(\boldsymbol{r}) - \boldsymbol{\rho}\cdot\nabla f^{\rm M}_{\rm i,gc}(\boldsymbol{r}) + \delta f_{\rm i,gc}(\boldsymbol{r}). \end{aligned} \tag{3}$$

Here $\boldsymbol{r}$ is the particle position, $\boldsymbol{R}$ the guiding center position, $\boldsymbol{\rho} = \boldsymbol{R} - \boldsymbol{r}$ the gyro-radius vector, and subscript 'gc' denotes guiding center distributions. We model here deuterium ions and neutrals (electron dynamics are negligible due to the small electron-ion mass ratio) and iterate to find the radial electric field which makes the momentum flux due to neutrals vanish.

In the case of the local drift kinetic equation (as defined, for example, in Ref. [22]), the system is linear; further, once we solve for the self-consistent electric field the toroidal velocity is proportional to the temperature gradient. The reason for this is that to solve the drift kinetic equation for δf, the inputs on the right hand side of the equation are the gradients of density, temperature, and electrostatic potential Φ. Since the $\partial n_{\rm i}/\partial\psi$ and $\partial\Phi/\partial\psi$ terms have identical velocity space structures, any density gradient is just offset by $\partial\Phi/\partial\psi$ without affecting δf and hence without affecting the flow. Since the only effect of the density gradient is to give a constant offset to the electric field, we set $\partial n_{\rm i}/\partial\psi = 0$. Since we solve for the electric field, the only driving term is the ion temperature gradient. The system is thus fully specified and so the toroidal rotation is determined.

We explore the effects of X-point position and shaping parameters, using model magnetic geometries given by analytic solutions to the Grad-Shafranov equation [23], with ITER-like parameters. These analytical solutions allow for arbitrary inverse aspect ratio ϵ, elongation κ,

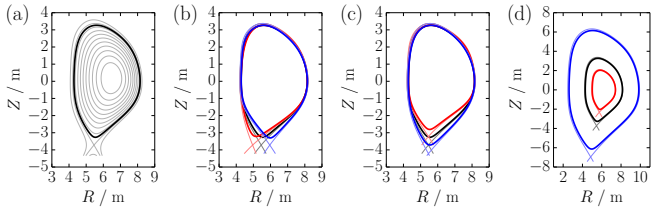

FIG. 1. Flux surface shapes: (a) baseline ITER equilibrium, (b) changing the major radius of the X-point R_X, (c) changing the vertical position of the X-point Z_X, and (d) changing the inverse aspect ratio ϵ. Thick lines show the $\psi_N = 0.95$ surface used for simulations.

triangularity δ, and X-point position. The geometry is specified by fixing the shape of the boundary surface in terms of ϵ, κ, δ, and X-point position major radius R_X and height Z_X. Two more constraints are also needed. We take the toroidal β, $2\mu_0\langle p\rangle/B_0^2$ (where $\langle p\rangle$ is the volume averaged pressure), to be 0.05 and fix the safety factor q_{95} of the flux surface with $\psi_N = 0.95$, where ψ_N is the normalized poloidal flux, to the value that corresponds to a plasma current of 15 MA in the baseline equilibrium. Scales are set by giving R_0, the major radius of the plasma center, and B_0, the vacuum toroidal field at R_0. The baseline parameters are [23]: $R_0 = 6.2$m, $B_0 = 5.3$T, $\epsilon = 0.32$, $\kappa = 1.7$, $\delta = 0.33$, $R_X = (1 - 1.1\delta\epsilon)R_0$, $Z_X = -1.1\kappa\epsilon R_0$. The variation of the X-point position and inverse aspect ratio, while keeping the other shaping parameters fixed, is illustrated in Fig. 1.

Clearly there is a rich parameter space of edge physics to explore with this numerical approach, with the plasma collisionality, the spatial distribution of the neutral density and the magnetic geometry all influencing the solutions. Our numerical tool allows these effects to be taken into account simultaneously. We also find good agreement with analytical results [18, 19] in the appropriate limits.

It is interesting to investigate the consequences of varying the position of a localized concentration of neutrals. The neutrals may be localized at a particular poloidal position, representing the location of a gas puff. They may also be concentrated near the X-point when the recycling from the targets is strong [14, 24], or if the plasma is gas fueled from the private flux region. Therefore we consider two scenarios. Firstly we vary the poloidal location of the neutrals in the baseline geometry and secondly vary the geometry in various ways while keeping the neutrals fixed at the X-point. In all cases we consider a single flux surface at $\psi_N = 0.95$, as highlighted with thick lines in Fig. 1.

The results show that the toroidal flow and electric field are largely determined by the major radius where the neutrals are localized, R_n, and the plasma collisionality. This is illustrated in Fig. 2, where we show the toroidal ion flow and radial electric field as a function

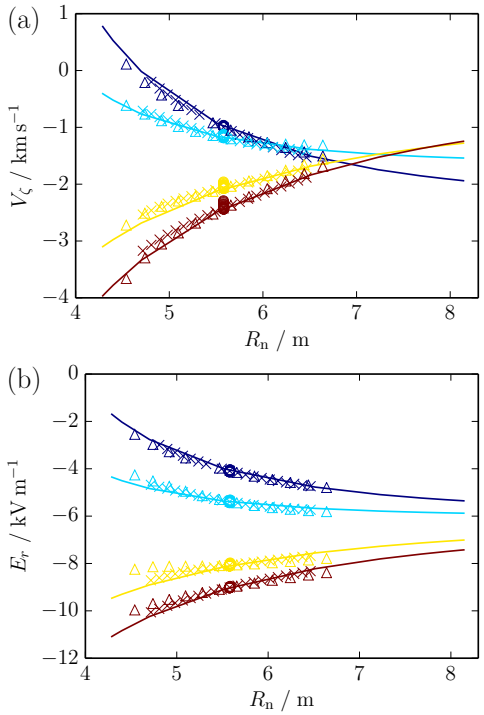

FIG. 2. (a) Toroidal flow velocity and (b) radial electric field at the outboard midplane as a function of the major radius where the neutrals are localized. Lines show the effect of changing the poloidal position of neutrals in the baseline geometry. Markers show the effect, with neutrals kept fixed at the X-point, of changing the geometrical parameters R_X (crosses), Z_X (circles), and δ (triangles). Line colors correspond to collisionality: cyan is the baseline corresponding to $n_i = 10^{20}$ m^{-3} and $T_i = 300$ eV, blue is 10 times lower, and yellow and red are 10 and 100 times higher respectively. The ion temperature scale length is taken to be 10 cm.

of the major radius where the neutrals were located, for various collisionalities. We show scans of the major radius of the X-point R_X, height of the X-point Z_X, and triangularity δ, all of which have the neutrals located at the X-point. We also scanned the poloidal location θ of the neutrals in the baseline equilibrium ($\theta = 0$ corresponding to the largest R_n, at the outboard midplane, and $\theta = \pi$ to the smallest, at the inboard midplane). Since the scans in θ, R_X, Z_X, and δ collapse on a single curve, we can see that the position of the X-point and triangularity affect the flow only by changing R_n, while the details of changes to the flux surface geometry are much less significant. One way to imagine controlling the major radius where the neutrals are localized is by changing the major radius of the X-point, and another is with the fueling location.

In contrast, the lowest order shaping parameters (inverse aspect ratio ϵ and elongation κ) have an effect on the flow and electric field that is not just described by R_n as in Fig. 2. Figure 3 shows that as ϵ varies there is an extremum in the toroidal flow. The collisionality de-

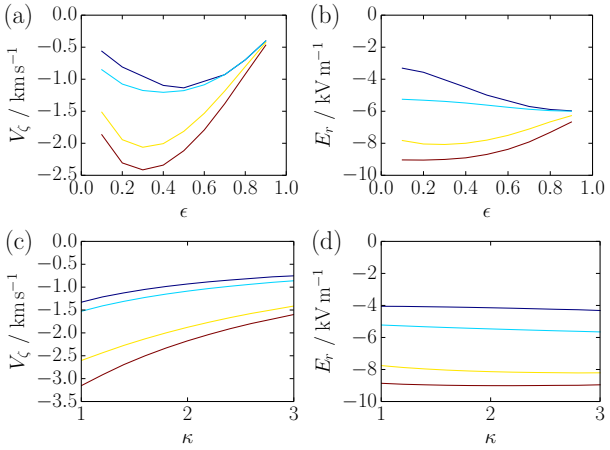

FIG. 3. (a) Toroidal flow velocity and (b) radial electric field at the outboard midplane for several inverse aspect ratios ϵ. (c) and (d) the same for elongations κ. Line colors correspond to collisionalities as in Fig. 2. The ion temperature scale length is again taken to be 10 cm.

pendence of both flow and electric field is suppressed for large ϵ. κ does not affect the electric field much, but the toroidal rotation decreases in magnitude as κ increases, as shown in Fig. 3.

The neutrals cause the plasma to rotate toroidally even in the absence of external momentum input. This is due to the fact that toroidal flow is needed to give a radial momentum flux balancing that due to the toroidal heat flux, which is present because of the radial temperature gradient [19]. In the limits $R_\mathrm{n} \to \infty$ in Fig. 2 and $\epsilon \to 1$ in Fig. 3 the electric field E_r approaches -6 kV m^{-1} $= -2T_i/(eL_{T_i})$, where L_{T_i} is the gradient scale length of the ion temperature. This is because in these limits only the rigid rotation parts of the flow and heat flux contribute to drive the radial momentum flux and these depend only on the radial gradients, not on $\delta f_{\mathrm{i,gc}}$; they are therefore independent of collisionality and so is the electric field which is set directly. The plasma flow in the $R_\mathrm{n} \to \infty$ limit does also have a contribution from the part of the flow parallel to the magnetic field (the part governed by the neoclassical coefficient k) and so does depend slightly on collisionality. It does not contribute to the momentum flux because $B(R_\mathrm{n}) \to 0$ in this limit. It is also notable that the trends in V_ζ and E_r with R_n (Fig. 2) reverse their direction as the collisionality changes from low to high. This follows from the change in sign of the neoclassical flow coefficient k between low (banana) and high (Pfirsch-Schlüter) collisionalities.

We find that the toroidal flow caused by the neutrals is generally counter-current and stronger for higher collisionality. The magnitude of the rotation in JET L-mode plasmas without external torque (without NBI heating) may be a few krad s^{-1}, corresponding to outboard velocities of order 10 km s^{-1} at a major radius of 3.7 m [25]; thus the speeds of a few km s^{-1} found here are of the same order of magnitude and at least likely to compete with other effects driving intrinsic edge rotation. The electric field is always inwards and is also stronger for higher collisionality. The effect of collisionality is enhanced when the neutrals are located at smaller major radii.

Allowing higher neutral densities requires including the reaction of the ion distribution to the neutrals [16], which will be implemented numerically in the future. PERFECT has the capability to include finite orbit width effects [22, 26], allowing density pedestals to be modeled and the study of the interaction between neutral momentum transport and pedestals is of the highest importance. The importance of and interaction with other effects such as ion orbit loss [27, 28] could also be considered.

Summary. We have built a framework to investigate the toroidal rotation and radial electric field in the edge plasma, when these are regulated through momentum transport by neutrals, by coupling neutrals to a neoclassical kinetic solver. Experimentally relevant parameters are not described by the asymptotic collisionality limits that can be studied analytically [16–20], which cannot, for intermediate collisionality, predict even the qualitative trends that should be expected. Intermediate collisionality is typical of experiments, see the cyan curves for baseline parameters in Figs. 2 and 3. Therefore quantitative comparison with experiment and predictive power for future devices both require the numerical solutions that we present here.

We find that the most important parameters that control the toroidal flow and electric field are the major radius where the neutrals are localized, R_n, and the plasma collisionality. These results suggest that altering the X-point position may offer a means to manipulate the edge rotation in the layer inside the separatrix where neutral viscosity dominates. This sets the boundary condition for the core rotation profile and influences the stability of magnetohydrodynamic instabilities such as resistive wall modes. Further, shear in the edge rotation can lead to the suppression of edge turbulence. Consequently the neutrals are also likely to affect the L-H transition and H-mode confinement. Our results demonstrate that the effects of neutrals on momentum transport are significant and should be accounted for both in the interpretation of current experiments and in the design of future machines.

The authors are grateful to Sarah Newton for useful discussions and to Matt Landreman for advice and help with the PERFECT code. This work was supported by the Framework grant for Strategic Energy Research (Dnr. 2014-5392) and the International Career Grant (Dnr. 330-2014-6313) from Vetenskapsrådet.

[1] E. Joffrin, J. Garcia, P. Tamain, E. Belonohy, H. Bufferand, P. Buratti, C. Challis, E. Delabie, P. Drewelow, D. Dodt, *et al.*, in *25th IAEA Fusion Energy Conference (FEC 2014)* (2014).

[2] P. Tamain, E. Joffrin, H. Bufferand, A. Jarvinen, S. Brezinsek, G. Ciraolo, E. Delabie, L. Frassinetti, C. Giroud, M. Groth, B. Lipschultz, P. Lomas, S. Marsen, S. Menmuir, M. Oberkofler, M. Stamp, S. Wiesen, and the JET EFDA contributors, Journal of Nuclear Materials **463**, 450 (2015).

[3] B. A. Carreras, L. W. Owen, R. Maingi, P. K. Mioduszewski, T. N. Carlstrom, and R. J. Groebner, Physics of Plasmas **5**, 2623 (1998).

[4] L. W. Owen, B. A. Carreras, R. Maingi, P. K. Mioduszewski, T. N. Carlstrom, and R. J. Groebner, Plasma Physics and Controlled Fusion **40**, 717 (1998).

[5] P. Gohil, L. R. Baylor, T. C. Jernigan, K. H. Burrell, and T. N. Carlstrom, Phys. Rev. Lett. **86**, 644 (2001).

[6] R. L. Boivin, J. A. Goetz, A. E. Hubbard, J. W. Hughes, I. H. Hutchinson, J. H. Irby, B. LaBombard, E. S. Marmar, D. Mossessian, C. S. Pitcher, J. L. Terry, B. A. Carreras, and L. W. Owen, Physics of Plasmas **7**, 1919 (2000).

[7] A. R. Field, P. G. Carolan, R. J. Akers, E. R. Arends, K. Axon, R. J. Buttery, N. J. Conway, G. F. Counsell, G. Cunningham, S. J. Fielding, M. Gryaznevich, A. Kirk, I. P. Lehane, B. Lloyd, M. A. McGrath, H. Meyer, C. Ribeiro, A. Sykes, A. Tabasso, M. R. Tournianski, M. Valovic, M. J. Walsh, H. R. Wilson, and the MAST & NBI Teams, Plasma Physics and Controlled Fusion **44**, A113 (2002).

[8] M. Valovic, P. G. Carolan, A. R. Field, S. J. Fielding, P. B. Jones, B. Lloyd, H. Meyer, M. Price, V. Shevchenko, K. Stammers, M. J. Walsh, S. You, and the COMPASS-D & ECRH Teams, Plasma Physics and Controlled Fusion **44**, A175 (2002).

[9] T. Fukuda, T. Takizuka, K. Tsuchiya, Y. Kamada, and N. Asakura, Plasma Physics and Controlled Fusion **42**, A289 (2000).

[10] A. R. Field, P. G. Carolan, N. J. Conway, G. F. Counsell, G. Cunningham, P. Helander, H. Meyer, D. Taylor, M. R. Tournianski, M. J. Walsh, and the MAST Team, Plasma Physics and Controlled Fusion **46**, 981 (2004).

[11] R. Maingi, C. S. Chang, S. Ku, T. Biewer, R. Maqueda, M. Bell, R. Bell, C. Bush, D. Gates, S. Kaye, H. Kugel, B. LeBlanc, J. Menard, D. Mueller, R. Raman, S. Sabbagh, V. Soukhanovskii, and the NSTX Team, Plasma Physics and Controlled Fusion **46**, A305 (2004).

[12] P. W. Terry, Rev. Mod. Phys. **72**, 109 (2000).

[13] P. J. Catto, P. Helander, J. W. Connor, and R. D. Hazeltine, Physics of Plasmas **5**, 3961 (1998).

[14] T. W. Versloot, P. C. de Vries, C. Giroud, M. Brix, M. G. von Hellermann, P. J. Lomas, D. Moulton, M. O. Mullane, I. M. Nunes, A. Salmi, T. Tala, I. Voitsekhovitch, K.-D. Zastrow, and the JET EFDA Contributors, Plasma Physics and Controlled Fusion **53**, 065017 (2011).

[15] T. Stoltzfus-Dueck, A. N. Karpushov, O. Sauter, B. P. Duval, B. Labit, H. Reimerdes, W. A. J. Vijvers, Y. Camenen, and the TCV Team, Phys. Rev. Lett. **114**, 245001 (2015); Physics of Plasmas **22**, 056118 (2015).

[16] T. Fülöp, P. J. Catto, and P. Helander, Physics of Plasmas **5**, 3398 (1998); Physics of Plasmas **5**, 3969 (1998).

[17] T. Fülöp, P. J. Catto, and P. Helander, Physics of Plasmas **8**, 5214 (2001).

[18] T. Fülöp, P. Helander, and P. J. Catto, Phys. Rev. Lett. **89**, 225003 (2002).

[19] P. Helander, T. Fülöp, and P. J. Catto, Physics of Plasmas **10**, 4396 (2003).

[20] A. N. Simakov and P. J. Catto, Physics of Plasmas **10**, 398 (2003).

[21] M. A. Dorf, R. H. Cohen, A. N. Simakov, and I. Joseph, Physics of Plasmas **20**, 082515 (2013).

[22] M. Landreman, F. I. Parra, P. J. Catto, D. R. Ernst, and I. Pusztai, Plasma Physics and Controlled Fusion **56**, 045005 (2014).

[23] A. J. Cerfon and J. P. Freidberg, Physics of Plasmas **17**, 032502 (2010).

[24] J. Callen, R. Groebner, T. Osborne, J. Canik, L. Owen., A. Pankin, T. Rafiq, T. Rognlien, and W. Stacey, Nuclear Fusion **50**, 064004 (2010).

[25] L.-G. Eriksson, T. Hellsten, M. F. F. Nave, J. Brzozowski, K. Holmström, T. Johnson, J. Ongena, K.-D. Zastrow, and JET-EFDA Contributors, Plasma Physics and Controlled Fusion **51**, 044008 (2009).

[26] I. Pusztai, S. Buller, and M. Landreman, Submitted to Plasma Physics and Controlled Fusion, arXiv:1603.00688 (2016).

[27] M. A. Dorf, M. R. Dorr, J. A. Hittinger, R. H. Cohen, and T. D. Rognlien, Physics of Plasmas **23**, 056102 (2016).

[28] T. Stoltzfus-Dueck, Phys. Rev. Lett. **108**, 065002 (2012); Physics of Plasmas **19**, 055908 (2012).